Inelastic neutron scattering study on different grades of palladium of varying pretreatment

2000 J. Phys.: Condens. Matter 12 4451

(http://iopscience.iop.org/0953-8984/12/20/301)

J. Phys.: Condens. Matter **12** (2000) 4451–4463. Printed in the UK PII: S0953-8984(00)11233-0

Inelastic neutron scattering study on different grades of palladium of varying pretreatment*

P Albers†‖, M Poniatowski†, S F Parker‡ and D K Ross§

† Degussa-Hüls AG, PO Box 1345, D-63403 Hanau, Germany
‡ ISIS Facility, Rutherford Appleton Laboratory, Chilton, Didcot OX11 0QX, UK
§ Department of Physics, University of Salford, Joule Laboratory, Salford M5 4WT, UK

E-mail: peter.albers@degussa-huels.de

Received 21 January 2000, in final form 14 March 2000

Abstract. The inelastic incoherent neutron scattering (IINS) technique has been utilized to study the way in which various kinds of palladium retain hydrogen after different pretreatments. Cold-rolled palladium foil, coarse palladium powder and finely divided palladium samples of different particle size and pretreatment were compared after controlled hydrogenation at room temperature and subsequent short-term dehydrogenation at 20, 50 and 70 °C. In a set of experiments under constant conditions, the incomplete decomposition of the β- and α-hydride phases at the given temperatures were found to be uncorrelated to the morphology of the samples under investigation or to the presence of strongly adherent carbonaceous degradation products at the surface of some of the samples. The dominant factor was the effect of hydrogen trapping due to mechanical pretreatment. It was shown that this effect may also be of some relevance at elevated temperatures.

It was also found that IINS is a suitable technique for the analysis of strongly adherent carbons at the surface of metals and metal hydrides and to discriminate between simple molecular structures and organic species of extended size. This is even the case for partial coverage of finely divided powders, the strong electromagnetic absorption and high electrical conductivity raises problems in utilizing other analytical techniques.

1. Introduction

Pure palladium and palladium-based materials are commonly used in various areas of technology. In addition to the well known application of this precious metal in decoration and jewellry palladium is used, for example, in the electronics industry for the production of multilayer capacitors or as a component in galvanic processes for the production of lead frames and electrical contact elements [1]. A very important field is the production of palladium-based heterogeneous and homogeneous catalysts. Palladium catalysts are used in different fields of petroleum refining such as the hydrofining process of fluidized catalytic cracking (FCC) or catalytic reforming [2], or in the reduction of acetylene to ethylene [3]. Another large-scale application with steadily growing importance is the introduction of palladium into modern automotive exhaust gas catalysts as an essential catalytic component of the 'washcoat' materials [4–6].

With respect to the great technological importance of palladium in catalytic hydrogenation reactions, the hydrogen-related properties such as hydrogen storage, surface activation and

* This paper is dedicated to Professor Dr Gerald Sicking on the occasion of his 60th birthday.
‖ Author to whom correspondence should be addressed.

0953-8984/00/204451+13$30.00

diffusion phenomena have been studied in detail ([7–11] and literature cited therein). The importance of hydrogen effects in catalysis has been summarized and reviewed in an authoritative survey [12].

There is still an important need to understand the different possible reasons for premature deactivation of palladium catalysts when used for organic syntheses. Palladium is not only able to store hydrogen, but may also incorporate carbon [13] and, indeed, is catalytically active in the transformation of amorphous carbon into aromatic/graphitic carbon [14–17] and may exhibit strongly bound molecular species at its surface [18].

In the deactivation of Pd catalysts, one has to consider not only chemical surface poisoning due to agents such as carbon monoxide or sulfidic sulfur or due to catalyst coking, but also that physical changes due to sintering or cold-working may well play an important role. It has been reported that under the influence of hydrogen, sintering of finely dispersed Pd can occur even at temperatures as low as 330 K [19]. Furthermore, enhanced mechanical stress or cold working [20] applied to the β-phase of palladium hydride may also cause particle growth and can lead to an enhanced defect density such as dislocations in the precious metal [21–24]. This may result in pronounced hysteresis effects of the hydrogen adsorption/desorption isotherms or the kinetics of hydrogen storage and release [7, 8, 20].

It is well known that the mechanical properties of Pd and Pd black change sequentially during hydrogenation from low concentrations (α-phase) over the α–β phase transition up to the fully loaded β-phase [7]: α-phase material is still quite hard, whereas under certain conditions the β-phase hydride can appear as a soft material which may tend to form agglomerates. Therefore, not only the catalytic properties, but also the mechanical changes in the supported and unsupported Pd particles have to be considered in applications where hydrogen is present. The physical and morphological changes due to hydrogenation may also be of some relevance in applications where not only the surface related properties of the Pd, such as the purity and the free area of the surface, are of importance but also where the hydrogen reversibly stored in the Pd particles might influence the catalytic properties. As is known from various studies on metal/hydrogen systems ([24] and literature cited therein) the release of stored hydrogen may be slowed significantly due to surface poisoning and hydrogen trapping effects. A decrease in the hydrogen mobility and the related inhibition in the phase transfer of hydrogen between bulk, selvedge and surface in the Pd and its transfer to reactants in the gas or liquid phases, may lead to a drop of the overall catalytic activity of the Pd. This aspect seems to deserve some additional attention.

In various studies it has been shown that inelastic neutron scattering (INS) is ideally suited to investigations of the metal/hydrogen system, for example [25–33]. For neutrons, the inelastic scattering is determined by the total scattering cross section and the amplitude of hydrogen vibration. For palladium, its large mass (106.4 amu) and small scattering cross section (4.48 barns, 1 barn $= 1 \times 10^{-28}$ m^2) mean that palladium is largely transparent to neutrons. In contrast, the incoherent scattering cross section for hydrogen (79.90 barns) together with its light mass (1.007 amu) ensures that the inelastic scattering is dominated by the hydrogenous motions.

Most of the detailed work on hydrogen dynamics for example [25–33], and the trapping of hydrogen on dislocations ([20–24] and literature cited therein) in the Pd/H system and other metal/hydrogen systems was focused on pure and well defined material such as single crystals or other bulk specimens with well determined preconditioning. In the present study, we have extended these existing neutron measurements on the palladium/hydrogen system, to several specimens of palladium of different morphologies, surface areas and pretreatments. The objective was to use the vibrational features of the protons as a direct local probe of the relevant properties of the palladium samples after hydrogenation and controlled dehydrogenation at different

temperatures. We wanted to investigate whether or to what extent, partial disorder, particle growth, or the presence of carbonaceous contamination may be of influence on hydrogen-related catalytic properties of this element which can therefore be studied by means of IINS.

2. Experimental details

2.1. Pd samples

The following palladium materials of different morphology and pretreatment were selected for preparing the samples used in the INS experiments (table 1).

Table 1. Palladium samples and sample weights.

Sample	Shape	Pretreatment	*In situ* measurement/3 min dehydrogenation	Weight (g)	Sample can diameter (cm)
1	Pd foil	Cold rolled	Dehydrogenation at 20 °C	48.4	2.5
1			Dehydrogenation at 50 °C		
1			Dehydrogenation at 70 °C		
2	Pd powder	Milled	Dehydrogenation at 50 °C	99.62	2.5
2			Dehydrogenation at 70 °C		
3	Pd black	Aged at 20 °C	Dehydrogenation at 20 °C	14.43	2.5
4			Dehydrogenation at 50 °C	43.45	2.5
5			Dehydrogenation at 70 °C	64.42	4.5
6	Pd black	Aged at 70 °C	Fully hydrogenated	33.61	2.5
7			Dehydrogenation at 20 °C	43.61	2.5
7			Second dehydrogenation at 20 °C		
8	Pd black	Aged at 50 °C	Fully hydrogenated	11.58	2.5
9			Dehydrogenation at 20 °C	23.295	

(A) Cold-rolled Pd-foil (sample 1). To study the INS spectrum of Pd with an enhanced concentration of dislocations and lattice strain as a bulk reference for disordered material, a piece of Pd (99.9%, Degussa) was cold rolled to a foil of 50 × 460 × 0.175 mm at room temperature. The surface was thoroughly cleaned by washing with petroleum ether (Merck, *pro analysi*) at room temperature to remove residual surface contamination. The efficiency of the purification procedure was finally monitored by means of x-ray photoelectron spectrometry (XPS). Only 26 at% of mainly aliphatic residual carbon was observed in the topmost atomic layers which could easily be removed by 5 min of 5 keV Ar^+ ion bombardment at 3 μA.

(B) Pd powder (sample 2). A commercial, coarse, Pd powder (purity 99.95%, Degussa) with a nitrogen surface area below 0.5 $m^2\ g^{-1}$ was measured as a disperse but low surface area counterpart of the bulk sample 1 (table 1). The numerical value of the surface area given, however, is only suitable for rough comparison because the application of the evaluation routines according to Brunauer, Emmet and Teller (BET) and related algorithms are of limited accuracy under these conditions. The sample was prepared by milling and it has, therefore, also experienced mechanical stress and shear forces.

(C) Precipitated Pd (samples 3–9). Three different Pd blacks (99.95%) prepared by a conventional liquid phase precipitation technique were selected, according to their different nitrogen surface areas resulting from different pretreatments. These samples were derived from freshly prepared commercial black material (48 $m^2\ g^{-1}$). Samples 3–5, 6, 7, 8 and 9 (section 2.2, table 1). They were prepared from the original black material by treatment at different temperatures for different times. They were suspended in organic solvents (raw mixtures of aromatic molecules including toluenes and benzenes) of technical quality in

conventional stirred gas/liquid hydrogenation reaction vessels. During the suspension process, the hydrogen pressure was varied in the range between 1.5 bar and a few mbar. The treatment was performed at 20 °C (preparing samples 3–5), 50 °C (preparing samples 8 and 9) and 70 °C (material for preparing samples 6 and 7) under 1.5 bar of hydrogen pressure to simulate the conditions for slow or enhanced particle growth at elevated temperatures [19] under varying hydrogen pressure and under the influence of organic material together with the conditions of intensive stirring and, therefore, interparticle contacts.

The treatment at 20 °C did not change the material significantly. Stirring at 50 °C (samples 8 and 9) caused a decrease of the nitrogen surface area of the material from 48 $m^2\ g^{-1}$ down to 17 $m^2\ g^{-1}$. The treatment at 70 °C led to material with a final surface area of 7.1 $m^2\ g^{-1}$.

Afterwards, samples 3–9 were thoroughly washed with acetone (Merck, *pro analysi*) at room temperature under exactly the same conditions to remove weakly adsorbed surface contamination or hydrogen-containing species whose scattering contributions might interfere with the hydrogenous scattering of the palladium-related hydrogen during the INS experiments.

Before preparing the samples for the INS experiments, their surface properties were checked by means of wide area XPS and secondary-ion mass spectrometry (SIMS). The presence of typical surface contaminants such as sulfidic sulfur or significant traces of metallic contaminants etc was ruled out. However, residual amounts of non-extractable carbon were detected on samples 6–9 in spite of the cleaning procedure. For samples 6 and 7 the evaluation of the XPS C1s signal (relative sensitivity factor 0.2) revealed a surface-carbon concentration of 65 at%. For samples 8 and 9, a value of 85 at% of residual carbon was found. A detailed analysis of the fine structure and asymmetry of the C1s peak together with the presence of a weak $\pi\pi^*$ shake-up satellite signal gave evidence of the presence of aromatic molecules. These carbonaceous layers could not be removed by repeated cycles of 15 min of surface erosion by means of 5 keV Ar^+ ion bombardment whereas in the case of samples 1-5 about 3–5 min of argon sputtering was sufficient to largely remove residual carbon contamination from the topmost atomic layers. Attempts to identify the chemical nature of these carbon residues in more detail by means of Fourier transform infrared spectroscopy (even attenuated total reflection (ATR) techniques with C- and Ge-crystal, respectively) and Raman spectroscopy, however, failed due to the high absorbance of the materials in spite of their coarse appearance compared to the original black. This limitation is also a problem in the characterization of supported precious metal catalysts such as Pd/C and can only be circumvented by neutron spectroscopy. The carbon content of the samples after cleaning was determined by elemental analysis: 0.7 wt% was observed for samples 6 and 7 and 1.4 wt% for samples 8 and 9 whereas the carbon values of the other specimens of palladium were below 0.05 wt%.

2.2. INS measurements

The INS spectra were measured with the TFXA-spectrometer (Time Focused Crystal Analyzer) and its successor, TOSCA, at the spallation neutron source ISIS (Rutherford Appleton Laboratory, UK). The resolution was ∼3% in $\Delta E/E$ and even better for TOSCA at lower energy transfer. The beam size was about 5 cm × 2 cm so that a representative macroscopic amount of a sample could be monitored. The samples were loaded into a closed-cycle refrigerator. The INS measurements were performed at 30 K.

The Pd samples were filled into He-leak-tested, thin-walled Al cans which were sealed by O-rings (Kalrez®, DuPont) and a welded bellows valve (Nupro). Empty can runs were performed on both TFXA and TOSCA to rule out any background contributions to the INS spectra of the palladium hydrides.

The samples in the cans were connected to a gas volumetric system and were pumped down to 10^{-5} mbar by means of a turbomolecular pump (Leybold Turbovac 50) backed by a two-stage rotary pump with a zeolite-containing adsorption trap to eliminate any contamination by aliphatics from backdiffusion from the pumping system. Afterwards they were carefully exposed to hydrogen (99.999%, Messer-Griesheim) at 22 °C with step-wise pressure increases ending with 1.5 bar of hydrogen pressure within 3 days. The hydrogen was then slowly removed in a subsequent dehydrogenation procedure, ending with the vacuum conditions of the turbomolecular pump. The dosing with the hydrogen and the hydrogen uptake in the range between 0.1 mbar (dilute α-Pd-hydride phase) up to about 1.5 bar (β-Pd-hydride phase) was controlled by a conventional gas volumetric method, as monitored by means of Baratron instruments (MKS 390HA, 227A and 220 BA). This cycle of hydrogenation/dehydrogenation was performed twice in total. The efficiency of the hydrogen uptake was determined by observation of the onset and the steep rise of the isotherms after conversion to the β-phase at n (H/Pd) $= 0.59$, in the $\sqrt{P}/n$ representation. The hydrogen isotherms obtained during the second cycle were already comparable to the literature data on conditioned Pd blacks with surface areas of 25–12 $m^2\ g^{-1}$ [34, 35]. However the width of the pressure plateau of the α–β transition region calculated from the gas volumetric data was narrowed because, under the chosen conditions, the short-term degassing of the samples at 22 °C was still incomplete. This interpretation was verified by additional hydrogen analysis in a separate set of experiments on degassed specimens of these samples using a LECO RH-404 hydrogen analyser. The H/Pd ratio of the degassed samples ranged between about 0.3 and 0.1, which is still in the range of the plateau region of the α–β phase transition [34, 35]. However, residual β as well as damaged α-phase hydride could both be present.

Care was taken to ensure that the hydrogen uptake was slow enough to avoid pronounced annealing of the samples by a quick release of the heat of solution of the hydrogen, which might have changed the properties of the specimens prior to the INS experiment to an uncontrolled extent. Previous SIMS spectra did not give evidence for the presence of water on the surfaces of the extracted blacks. SIMS cluster-ion signals for species such as $PdOH^+$ or $PdOH^-$ were only very weak. Nevertheless the hydrogen cycling procedure was chosen to also avoid any dominating influence of adsorbed species such as oxy-hydrates on the INS spectra.

A deliberate conditioning of the final Pd samples, by additional hydrogenation/dehydrogenation cycles at elevated temperatures to anneal out any disorder to establish the ideal conditions for measuring the well known shape of the hydrogen isotherms of ideally-activated, preconditioned Pd was beyond the scope of the present study.

The samples showed the usual rather fast hydrogen uptake without pronounced induction periods. This was even the case for the Pd foil; the use of a hydrogen transfer catalyst [34] or electrochemical preconditioning—essential for activating bulk specimens for their first hydrogen uptake—was not necessary for loading the bulk material. Presumably the lattice relaxation of the strained, cold-worked Pd foil during hydrogen uptake, the formation of the hydride and the α–β phase transition, are responsible for the spontaneous and fast hydrogen uptake of the bulk material, even at room temperature. The introduction of energy and strain into the specimen by the cold-rolling treatment was sufficient to activate the material.

The object of this study was to measure changes in the energies and relative intensities of the INS signals of the protons in the α- and β-hydride phases as a function of the morphology and the pretreatment. Therefore the INS spectra before and after controlled hydrogenation/dehydrogenation procedures at temperatures adequate for the given sample should be compared. For efficient use of the beam time, a series of separate gas volumetric experiments were performed separately to work out the conditions (pumping times, temperatures of dehydrogenation, etc) under which pronounced effects were to be expected for a given

palladium sample. Considering the results and the beam time allocation at ISIS, the samples were subjected to INS under the conditions given in table 1 and as summarized as follows.

The cold-rolled Pd foil (sample 1) was measured after dehydrogenation at 20, 50 and 70 °C; the sample was measured consecutively after repeated dehydrogenation (2.5 cm can).

The milled Pd powder (sample 2) was measured after dehydrogenation at 50 and 70 °C (2.5 cm can).

The Pd as-aged at 20 °C was measured after a 3 min dehydrogenation at 20 °C (2.5 cm can); a further sample was measured after 3 min of dehydrogenation at 20 °C and 3 min at 50 °C and, finally, a sample was measured after subsequent dehydrogenation at 20, 50 and 70 °C (samples 3–6). The aged black with enhanced particle size was measured under 1.5 bar H_2 equilibrium pressure and after one and two dehydrogenation treatments, both at 20 °C (samples 6 and 7). The aged black of lower particle size was measured under 1.5 bar H_2 equilibrium pressure and after one dehydrogenation treatment at 20 °C (samples 8 and 9).

The times of dehydrogenation were kept constant throughout the experiments (3 min for each individual treatment) as well as the pumping parameters of the system used. However, in spite of the well defined pumping conditions a quantitave evaluation of hydrogen desorption characteristics in terms of determining diffusion coefficients or a detailed evaluation of trap concentrations is beyond the scope of the present study and has to be achieved by other techniques (see, for example, [21, 22, 24]).

The sample weights are summarized in table 1. The INS spectra were normalized to the amount of material in the neutron beam after subtraction of an empty-can background. In the figures for clarity the spectra have been displaced along the y-axis. The displacements are given in brackets in the legend.

3. Results and discussion

The INS spectra of the Pd samples are compared in the figures 1–5. A selection of published INS data [25–33, 36–40] and data from other techniques [41–43] is compiled in table 2 as references for the following discussion.

The INS spectra of the cold-worked hydrogenated material which were obtained after dehydrogenation at 20 and 50 °C (figure 1, curve (a) and (b)) are dominated by a very strong signal in the range of 57–60 meV, which represents the local modes of the screened protons that are dissolved in the bulk metal, vibrating in the octahedral sites of the fcc lattice. The asymmetric broadening of the signal at about 70–90 meV is consistent with the results on β-phase Pd as reported in [26–29] (see table 2). It is suggested by Kemali *et al* [40] that the shoulder is due to a Franck–Condon level, an excited proton wavefunction established in a Pd lattice that has not relaxed from its equilibrium shape, with the proton in its first excited state. When the lattice relaxes to take account of the proton in its first excited state, the energy level drops and becomes narrower (longer lifetime) giving the sharp peak. This effect will influence comparisons with near-surface states or of the coupling between adjacent atoms of D [40] and H. An overtone of this fundamental β-hydride vibration appears at about 110 meV and a second weak overtone above 200 meV [33, 39]. A detailed outline of these signals including anharmonicity effects has been given in [39, 40]. The presence of the vibrational modes of the β-phase of palladium hydride even after dehydrogenation at 50 °C can be explained by the fact that a bulk-like material is measured and that, futhermore, the hydrogen diffusion is decelerated by the enhanced amount of imperfection due to the cold-rolling process. Trapping on dislocations/stacking faults will slow down diffusion but the trap sites will also be occupied at a lower chemical potential. Of course, H eventually pumps out but the chemical potential driving force will be lower in the disrupted lattice.

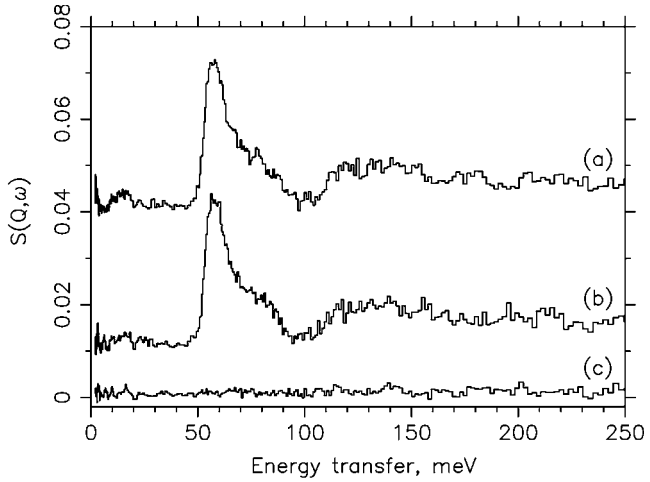

Figure 1. INS spectra of cold-rolled hydrogenated Pd foil (sample 1): curves (a) after 3 min of dehydrogenation at 20 °C, (+0.04); (b) as curve (A) after additional dehydrogenation for 3 min at 50 °C, (+0.01); and (c) as curve (B) after additional dehydrogenation for 3 min at 70 °C. Note that the figures in brackets refer to displacements along the y-axis, for clarity.

However, after a dehydrogenation at 70 °C, the hydrogen was largely expelled from the sample. Apparently complete decomposition of the β-phase as well as of the α-phase was achieved and the cold-rolled bulk material seems to be cured so far by the previous two cycles of hydrogen absorption and desorption and by the two short periods of thermal treatment such that the residual amounts of trapped hydrogen are below the detection limit of the spectrometer (figure 1 curve (c)). This is not the case for the coarse palladium powder, sample 2. Trapped hydrogen changes the repulsion energy between dislocations and therefore cycling causes them to move around and gradually unravel and disappear.

Figure 2 curve (a) shows that after the dehydrogenation at 50 °C, weak features of a signal due to superposition of the peak from β-phase hydride at about 58.8 meV and of α-hydride at about 71.2 meV are present. After the second dehydrogenation treatment (70 °C, figure 2 curve (b)) some residual signal intensity is still observed at 71.7 meV indicating the presence, and incomplete decomposition, of α-phase hydride which is already missing in figure 1 curve (c). Very weak features at about 115–118 meV may be attributed to the symmetric H stretching at the Pd surface [41–43].

The relative intensities of the vibrations of the Pd lattice show some variation of the relative intensities of these features with the amount of residual β- and α-phase hydride, respectively.

Figure 3 also shows residual hydride peaks for a freshly-precipitated, palladium-black material of comparatively high surface area after ageing at 20 °C. In spite of the shorter diffusion paths inside the particles, the decomposition of the hydride phases seems partly inhibited. After dehydrogenation at 20 °C the band of the β-hydride vibrational mode still dominates the spectrum (figure 3 curve (a)). After dehydrogenation at 50 °C a superposition of the vibrational features of the β-phase at 57.4 meV and, additionally, of the α-phase are measured (figure 3 curve (b)) with, however, significantly lowered intensity. After the second dehydrogenation step, features of α-phase (71.1 meV) and only traces of β-phase (around 59–60 meV) appear (figure 3 curve (c)).

The results from figures 1–3 indicate that for the present samples, the tendency to retain some residual hydrogen can be observed for cold-rolled bulk material as well as for the

Table 2. INS results on the palladium/hydrogen system as reported in literature.

Pd sample	Peak energy (meV)	Peak assignment	Additional features (meV)	Reference
Single crystal 0.2 at% H	66 ± 4	α-hydride	Shift to 63 at 2.7 at% H	[25]
Single crystal	135 ± 15	α-hydride second harmonic		[25]
Foil	57.5	β-phase	High-energy shoulder at 80–90, decreasing frequency with increasing H concentration	[26, 27, 31, 32]
Raney Pd	59.5 70.0	β-phase α-hydride	Overtone at 142.5; second overtone at 223; and additional features at 74.9, 89.2, 95.6 and 120.8	[33]
H on Pd (111)	96, 124			[43]
Pd (100)	101.9	Symmetric H stretching		[29, 33]
Pd (111)	113.5	Symmetric H stretching		[29, 33]
Pd (100), (111)	210.7	Asymmetric H stretching		[29, 33]
Pd black	69 58	α-hydride Subsurface hydrogen	94, 101, 120 weak: 75, 111, 180; 94, 101 and 120 increase with H-content	[8, 28, 42]
Pd in Y zeolite	70.6 59.5 86.7 122.7	α-hydride β-phase Subsurface hydrogen Chemisorbed hydrogen		[36]
Pd/activated carbon	55.8 75.6	β-phase α-hydride	102.8, 114.0	[37]
Pd/carbon black	56.0 76.8	β-phase α-hydride		[37]

dispersed Pd with surface areas of 0.5 $m^2\ g^{-1}$ produced by milling and 47 $m^2\ g^{-1}$ produced by precipitation. The materials have experienced or retained some mechanical stress according to their different pretreatment. Surprisingly this is not completely cured at 70 °C in the case of the finely divided materials (figure 2 curve (b) and figure 3 curve (c)) whereas complete release of stored hydrogen was observed for the foil (figure 1 curve (c)). It is remarkable that this finding cannot be explained by the presence of contaminating surface layers etc which are missing in the case of samples 1–5.

This finding may be explained by the presence of trap sites and suggests that the generation of traps in palladium is not solely induced by mechanical shear, but that finely divided material from a chemical production route may contain residual structures which are equally capable of trapping hydrogen or at least causing some retardation in its release.

It is possible that there are stronger forces tending to remove deformation damage in the bulk as compared to the powder form. Thermal annealing of the defects and a corresponding

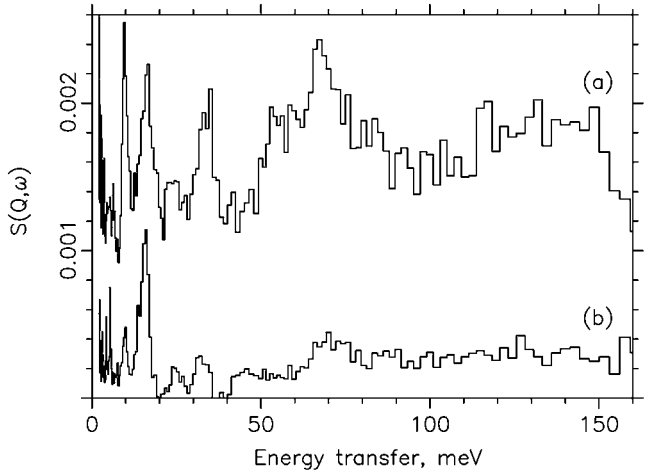

Figure 2. INS spectrum of hydrogenated Pd powder (sample 2): curves (a) after 3 min of dehydrogenation at 50 °C, (+0.001); and (b) as (a) after 3 min of additional dehydrogenation at 70 °C.

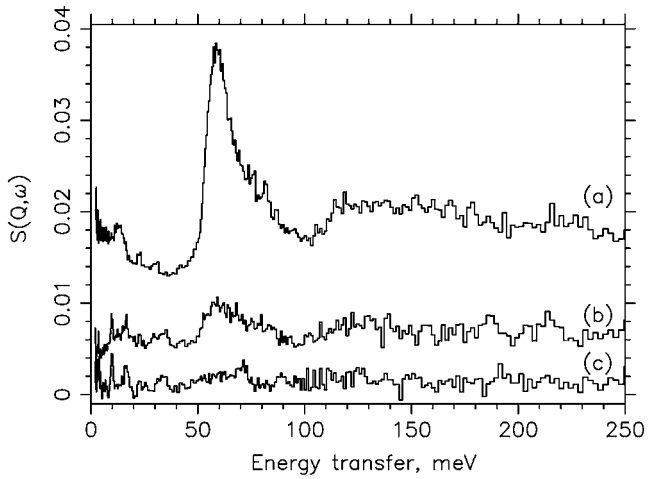

Figure 3. INS spectra of precipitated, aged (20 °C) hydrogenated Pd black (samples 3–5): curves (a) after 3 min of dehydrogenation at 20 °C (sample 3), (+0.01); (b) after 3 min of dehydrogenation at 20 °C and 3 min of dehydrogenation at 50 °C (sample 4), (+0.005); and (c) after 3 min of dehydrogenation at 20 °C, 3 min at 50 °C and 3 min at 70 °C (sample 5).

additional preconditioning by repeated cycles of hydrogenation and dehydrogenation seem necessary to obtain the well known sorption characteristics of finally activated palladium. Surprisingly it was found that the samples contaminated with non-extractable carbon species dehydrogenate rapidly at 20 °C in spite of having a comparatively low and partly covered surface area. Figure 4 shows that for the coarse material (7.1 $m^2\ g^{-1}$) a second dehydrogenation step is necessary whereas the second black with 15 $m^2\ g^{-1}$ shows a hydride decomposition within a single dehydrogenation step at 20 °C. However, in both cases, residual broad features remain in the spectral regions of 90–147 and 150–200 meV (figure 4 curve (c) and figure 5 curve (b)). In the fully-hydrogenated condition, these are presumably hidden by the broad

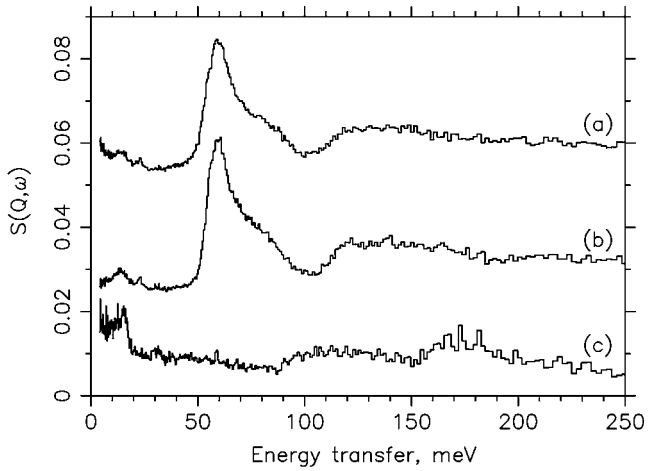

Figure 4. INS spectra of aged (70 °C) hydrogenated Pd black (samples 6 and 7): curves (a) recorded under 1.5 bar of hydrogen pressure (equilibrium pressure at 20 °C, sample 6), (+0.005); (b) after 3 min of dehydrogenation at 20 °C (sample 7), (+0.002); and (c) after additional 3 min of dehydrogenation at 20 °C (sample 7).

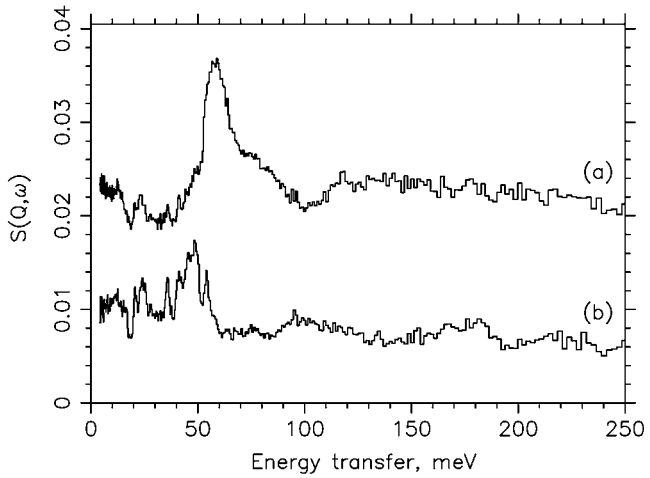

Figure 5. INS spectra of aged (50 °C) hydrogenated Pd black (samples 8 and 9): curves (a) recorded under 1.5 bar of hydrogen pressure (equilibrium pressure at 20 °C, sample 8), (+0.015); and (b) after 3 min of dehydrogenation at 20 °C (sample 9); (×4 ordinate expansion).

signal of the first overtone contributions from the octahedral site vibrations of the β-phase hydrogen (figure 4 curves (a) and (b) and figure 5 curve (a)). Clearly, these peaks cannot be attributed to the vibrations of H on the octahedral sites since the fundamental vibration is missing in these cases. These features are weak or largely missing for the case of the high-surface-area material as already seen from figure 3. This material had also been exposed to organic molecules, but at lower temperature. Possible interpretations of these features could be the presence of vibrations of hydrogen on tetrahedral sites or on trap sites. INS work on metal–hydrogen systems does reveal vibrations on tetrahedral sites which appear at the energies observed here (e.g. [44–47]). However, with respect to the given fcc lattice this

possibility seems unlikely. Krimmel *et al* [23], for instance, shows that tetrahedral sites have considerably higher energy. Trap sites, on the other hand, were shown to provide spacious, flat potential wells for hydrogen and, therefore, much lower vibrational frequencies [20, 40, 45]. The flatness of the bottom of the octahedral site is that minima would develop around the edge of the site which add together to give flat bottom of the potential well. The trap site might become more stable at larger lattice parameters, for example in sub-surface sites. Hence, to assign the broad bands to being signals due to trap-like interstitial positions of hydrogen also seems unlikely.

According to surface analyses by means of XPS and to investigations on the purity of the bulk material using elemental analysis and the x-ray fluorescence method, the only other prominent residual component in samples 6–9 is non-extractable carbon which is largely absent in samples 3–5. It would therefore appear that the broad bands in the ranges 90–145 and 150–200 meV (figure 4 curve (c) and figure 5 curve (b)) have to be assigned to C–H bending modes of sp^2- and sp^3-like species which strongly adhere to the palladium samples. This is supported by weak features appearing at about 370–400 meV which are typical of sp^2 and sp^3 C–H stretching modes [48]. The bands at 90–145 and 150–200 meV are due to polycondensed material or first degradation products, accumulated during the circulation of the palladium samples in the organic solvents during the ageing processes at elevated temperatures. These features were missing on samples 3–5 which were treated under similar conditions, but at considerably lower temperature. The average size of these entities is probably greater than 2 nm since no clear indications for the presence of the INS bands due to aromatic ring deformations were obtained which are known for structures such as those derived from heat-treated naphthalenes [49], molecules such as perylene [50], partly hydrogasified carbon blacks [51] or activated carbons [37]. These molecules could not be extracted by the acetone pretreatment prior to the INS experiment and are quite stable to common solvents.

Regarding the well known solution/precipitation mechanism [14, 15] that results in the conversion of amorphous carbon into graphitic structures under the catalytic influence of palladium, it may be assumed that these bands represent strongly adherent carbon as an intermediate in the degradation processes on the one hand and the catalytic conversion of amorphous into more crystalline carbon on the other.

Uniquely, vibrational features at 36, 41, 45, 50 and 54 meV are visible in figure 5 curve (b) which are assigned to rather well structured features of molecular-type vibrations. These are just visible in the fully-hydrogenated condition for this sample (figure 5 curve (a)), where they are partly hidden by the vibrations of the β-hydride and give rise to an asymmetric broadening at the low-energy edge of this peak. Because rather sharp and narrow vibrational bands are observed, this organic contribution to the overall carbon content is chemically connected to the Pd surface and consists of rather simple entities whereas the organic material of larger structures, as indicated by the broad bands at 90–145 and 150–200 meV, may be enclosed in intra- and interparticle porosity.

These sharp bands are interpreted as simple molecular species complexing some Pd atoms at the surface (the vibrations of metal–organic complexes or compounds appear below 50 meV) or to simple organic species which show multiplet splitting due to a geminal substitution and steric blocking of the free vibration. These bands do not represent hydrogen associated with dissolved carbon inside the Pd bulk [13] since they appear as very narrow signals. Figure 5 thus illustrates that strongly-adhering, hydrogen-containing organic molecules of molecular structure and of polycondensed structure on metal blacks can be discriminated between. This was not possible with conventional techniques such as Fourier transform IR or Raman spectroscopies.

4. Conclusions

INS has been applied here as a surface and a bulk related technique. It is uniquely valuable to study the hydrogen storage in and release from bulk-like α- and β-phase palladium hydrides. INS is also able to measure and to discriminate between small molecular-like entities or extended polycondensed carbonaceous systems which are strongly adherent to a palladium surface and which are not observable by other methods.

For the given set of palladium samples measured, the tendency to retain hydrogen in the bulk is much more dependent on the mechanical pretreament than to their morphology. The existence of partly enhanced numbers of trap sites due to these pretreatments may explain these observations. The presence of considerable amounts of strongly adherent organic surface contaminants or degradation products has virtually no influence on hydrogen storage and release of the metal hydride system.

In addition to the well known effect of particle growth, enhanced interactions between organic solvent molecules and the palladium surface may appear at elevated temperatures (50 and 70 °C) which can lead to carbonaceous deposits which are chemically bound to the metal surface and which are stable in air. However, preconditioning of palladium by repeated cycles of controlled hydrogenation/dehydrogenation seems sufficient to provide activated material, the hydogen uptake and release of which was not significantly hampered by organic adsorption layers.

Acknowledgments

The Rutherford Appleton Laboratory is thanked for access to neutron beam facilities. Stefan Zeuner is thanked for providing the cold-rolled palladium material.

References

[1] *Edelmetall Taschenbuch* 1995 ed Degussa AG Frankfurt (Heidelberg: Hüthig)
[2] Kirk-Othmer 1993 *Encyclopedia of Chemical Technology* 4th edn, vol 5 (New York: Wiley) p 342
[3] Müller H, Deller K, Vollheim G and Kühn W 1987 *Chem. Eng. Technol.* **59** 645
Deller K 1990 *Catalysis by Organic Reactions* ed D W Blackburn (New York: Dekker) p 301
[4] Taylor K C 1984 *Catalysis-Science and Technology* vol 5, ed J R Anderson and M Boudart (Berlin: Springer) p 141
[5] Engler B H, Lox E S, Ostgathe K, Ohata T, Tsuchitani K, Ichihara S, Onoda H, Garr G T and Psaras D 1994 *SAE-Paper* No 940928 (Warrendale, PA: Society of Automotive Engineers Inc.)
[6] Lindner D, Lox E S, vanYperen R, Ostgathe K and Kreuzer T 1996 *SAE Paper* No 960802 (Warrendale, PA: Society of Automotive Engineers Inc.)
[7] Lewis F A 1967 *The Palladium Hydrogen System* (London: Academic) p 23–30
[8] Wicke E and Brodowsky H 1978 *Hydrogen in Metals II (Topics in Applied Physics, vol 29)* ed G Alefeld and J Völkl (Berlin: Springer) p 73
[9] Sicking G 1972 *Ber. Bunsenges. Phys. Chem.* **76** 790
[10] Sicking G and Buchold H 1971 *Z. Naturforsch.* **26a** 1973
[11] Sicking G 1974 *Z. Physik. Chem.* **93** 53
[12] Paal Z and Menon P G (eds) 1988 *Hydrogen Effects in Catalysis—Fundamentals and Practical Applications* (New York: Marcel Dekker)
[13] Stachurski J and Frackiewicz A 1985 *J. Less-Common Met.* **108** 249
[14] Holstein L, Moorhead R D, Poppa H and Boudart M 1982 *Chem. Phys. Carbon* **18** 139
[15] Lamber R, Jäger N and Schulz-Ekloff G 1990 *Surf. Sci.* **227** 15
Lamber R, Jäger N and Schulz-Ekloff G 1988 *Surf. Sci.* **197** 402
[16] Krishnankutty N and Vannice M A 1995 *J. Catal.* **155** 312
[17] Albers P, Seibold K, Prescher G and Müller H 1999 *Appl. Catal.* A **176** 135
[18] Albers P, Angert H, Prescher G, Seibold K and Parker S F 1999 *Chem. Commun.* **17** 1619

[19] Sermon P 1972 *J. Catal.* **24** 460
Sermon P 1972 *J. Catal.* **24** 467
[20] Sicking G, Glugla M and Huber B 1983 *Ber. Bunsenges. Phys. Chem.* **87** 418
[21] Kirchheim R 1981 *Acta Met.* **29** 845
Kirchheim, R, Huang X Y, Carstanjen H D and Rush J J 1987 *NATO ASI Series (Series E, vol 130)* p 580
Kirchheim, R, Huang X Y, Carstanjen H D and Rush J J 1987 *Chem. Phys. of Fracture (Bad Reichenhall, June 23–July 1, 1987)* (Dordrecht: Martinus Nijhoff) pp 585–9
[22] Kirchheim R, Huang X Y and Muetschele T 1989 *Hydrogen Effects on Material Behaviour, Proceedings of the International Conference on the Effect of Hydrogen on the Behaviour of Materials, 4th, Miner. Met. Mater. Soc.* ed N R Moody and A W Thompson (Warrendale, PA: Minerals. Metals and Materials Society) p 847
[23] Krimmel H, Schimmele L, Elsässer C and Fähnle M 1994 *J. Phys.: Condens. Matter* **6** 7679
[24] Wert Ch 1978 *Hydrogen in Metals II (Topics in Applied Physics, vol 29)* ed G Alefeld and J Völkl (Berlin: Springer) p 305
[25] Drexel W, Murani A, Tocchetti D, Kley W, Sosnowska I and Ross D K 1976 *J. Phys. Chem. Solids* **37** 1135
[26] Ross D K, Martin P F, Oates W A and Khoda Bakhsh R 1979 *Z. Phys. Chem.* **114** 221
[27] Hunt D G and Ross D K 1976 *J. Less-Common Met.* **49** 169
[28] Nicol J M, Rush J J and Kelley R D 1987 *Phys. Rev.* B **36** 9315
Nicol J M, Rush J J and Kelley R D 1988 *Surf. Sci.* **197** 67
[29] Howard J, Waddington T C and Wright C J 1978 *Chem. Phys. Lett.* **56** 258
[30] Rowe J M, Rush J J, Smith H G, Mostoller M and Flotow H E 1974 *Phys. Rev. Lett.* **33** 1297
[31] Rahman A, Sköld K, Pelizzari C, Sinha S K and Flotow H E 1987 *Phys. Rev.* B **14** 3630
[32] Braid I J, Howard J and Tomkinson J 1983 *J. Chem. Soc., Faraday Trans. II* **79** 253
[33] Jobic H, Candy J-P, Perrichon V and Renouprez A 1985 *J. Chem. Soc., Faraday Trans. II* **81** 1955
[34] Wicke E and Nernst G H 1964 *Ber. Bunsenges. Phys. Chem.* **68** 224
[35] Frieske H and Wicke E 1973 *Ber. Bunsenges. Phys. Chem.* **77** 50
[36] Jobic H and Renouprez A 1987 *J. Less-Common Met.* **129** 311
[37] Albers P, Burmeister R, Seibold K, Prescher G, Parker S F and Ross D K 1999 *J. Catal.* **181** 145
[38] Ross D K, Stefanopoulos K L, Forcey K S and Iordanova I 1994 *Z. Phys. Chem.* **183** 29
[39] Ross D K, Antonov V E, Bokhenov E L, Kolesnikov A I, Ponyatovsky E G and Tomkinson J 1998 *Phys. Rev.* B **58** 2591
[40] Kemali M, Totolici J E, Ross D K and Morrison I 2000 *Phys. Rev. Lett.* **8** 1531
[41] Ratajczykowa I 1975 *Surf. Sci.* **48** 549
[42] Behm R J, Penka V, Cattania M G, Christmann K and Ertl G 1983 *J. Chem. Phys.* **78** 7486
[43] Conrad H, Kordesch M E, Scala R and Stenzel W 1986 *J. Electron Spectrosc. Related Phenom.* **38** 289
[44] Sicking G, Albers P and Magomedbekov E 1983 *J. Less-Common. Met.* **89** 373
[45] Benham M J, Browne J D and Ross D K 1984 *J. Less-Common. Met.* **103** 71
[46] Hempelmann R, Wicke E, Hilscher E and Wiesinger G 1983 *Ber. Bunsenges. Phys. Chem.* **87** 48
[47] Albers P, Sicking G and Ross D K 1989 *J. Phys.: Condens. Matter* **1** 6025
[48] Lin-Vien D, Colthup N B, Fateley W G and Grasselli J G 1991 *The Handbook of Infrared and Raman Characteristic Frequencies of Organic Molecules* (San Diego: Academic)
[49] Leung P S and Safford G J 1970 *Carbon* **8** 527
[50] Fillaux F, Papoular R, Lautié A and Tomkinson J 1994 *Carbon* **32** 1325
[51] Albers P, Seibold K, Prescher G, Freund B, Parker S F, Tomkinson J, Ross D K and Fillaux F 1999 *Carbon* **37** 437